Inventory of boreal fire emissions for North America in 2004: the importance of peat burning and pyro-convective injection

Solène Turquety[1], Jennifer A. Logan, Daniel J. Jacob, Rynda C. Hudman, Fok Yan Leung, Colette L. Heald[2], Robert M. Yantosca, Shiliang Wu
Department of Earth and Planetary Sciences and Division of Engineering and Applied Sciences, Harvard University, Cambridge, Massachusetts, USA

Louisa K. Emmons, David P. Edwards
Atmospheric Chemistry Division, National Center for Atmospheric Research, P.O. Box 3000, Boulder, CO

Glen W. Sachse
NASA Langley Research Center, Hampton, VA

[1] Now at Service d'Aéronomie, IPSL, Paris, France
[2] Now at Center for Atmospheric Sciences, University of California, Berkeley, CA

Abstract.

The summer of 2004 was one of the strongest fire seasons on record for Alaska and western Canada. We construct a daily bottom-up fire emission inventory for that season, including consideration of peat burning and high-altitude (buoyant) injection, and evaluate it in a global chemical transport model (the GEOS-Chem CTM) simulation of CO through comparison with MOPITT satellite and ICARTT aircraft observations. The inventory is constructed by combining daily area burned reports and MODIS fire hotspots with estimates of fuel consumption and emission factors based on ecosystem type. We estimate the contribution from peat burning using drainage and peat distribution maps for Alaska and Canada; 17% of the reported 5.1×10^6 ha burned were located in peatlands in 2004. Our total estimate of North American fire emissions during the summer of 2004 is 28.6 Tg CO, including 9.6 Tg from peat. Including peat burning in the GEOS-Chem simulation improves agreement with MOPITT observations. The long-range transport of fire plumes observed by MOPITT suggests that the largest fires injected a significant fraction of their emissions in the upper troposphere.

1 Introduction

Biomass burning represents a major global source of gases and aerosols to the atmosphere [*Seiler and Crutzen*, 1980; *Logan et al.*, 1981; *Crutzen and Andreae*, 1990; *Liousse et al.*, 1996; *Andreae and Merlet*, 2001]. Wildfires in the northern hemisphere boreal regions also have a significant impact on atmospheric chemistry on regional to global scales, particularly in high fire years [*Forster et al.*, 2001; *Wotawa et al.*, 2001; *Novelli et al.*, 2003; *Edwards et al.*, 2004; *Honrath et al.*, 2004; *van der Werf et al.*, 2004; *Yurganov et al.*, 2004; *Kasischke et al.*, 2005]. Air quality in the United States can be affected by emissions from fires in the boreal forests of Canada [*Wotawa and Trainer*, 2000; *McKeen et al.*, 2002; *DeBell et al.*, 2004] and even Siberia [*Jaffe et al.*, 2004]. Boreal fires also contribute to Arctic Haze [*Stohl et al.*, 2006a, 2006b]. An accurate representation of emissions from boreal wildfires is all the more necessary as their occurrence is expected to increase as a result of climate change [*Flannigan and Wagner*, 1991; *Stocks et al.*, 1998, 2003; *Whitlock*, 2004; *Gillett et al.*, 2004]. Intense burning causes a decrease of carbon storage in these ecosystems, which can be converted from a carbon sink to a net source, in turn contributing to global warming *[Kurz and Apps, 1999; Turetsky et al., 2002]*. In this study, we examine the consistency between current understanding of boreal fire emissions and satellite observations of carbon monoxide (CO) for the summer of 2004. For this purpose, we develop a detailed bottom-up inventory of the North American fire emissions in 2004 with daily variability and implement it in a global 3-D chemical transport model (the GEOS-Chem CTM) for comparison with atmospheric observations of CO.

The summer of 2004 was one of the largest fire seasons on record in North America, because of persistent wildfires in the boreal forests of Alaska and Canada. This intense burning resulted from exceptionally warm and dry conditions. According to the U.S. National Interagency Fire Center (http://www.cidi.org/wildfire), more than 2.6 million ha burned in Alaska in 2004, which represents more than 8 times the 10-year average and the highest burning on record, while the total area burned in the rest of the United States was only about 40% that of the 10-year average. In western Canada the fire season was well above the 10-year average, with 15 times the average area burned in the Yukon Territory (accounting for 60% of the national total) and 6 times the average area burned in British Columbia, according to the Canadian Interagency Forest Fire Center (CIFFC).

The availability of extensive atmospheric CO observations from aircraft and satellite for this period provides an opportunity to evaluate our understanding of factors controlling boreal fire emissions and their impact on atmospheric chemistry. Continuous observations of CO with global coverage every 3 days were made from the MOPITT (Measurements Of Pollution In The Troposphere) satellite instrument [*Drummond*, 1996; *Edwards et al.*, 1999; *Deeter et al.*, 2003; *Emmons et al.*, 2004]. Extensive in situ aircraft observations over eastern North America and the North Atlantic were made from July 1st to August 15th 2004 during the ICARTT (International Consortium for Atmospheric Research on Transport and Transformation) field campaign.

Earlier global emission inventories were based on average assessments of fire activity and areas burned [*Crutzen and Andreae*, 1990; *Hao and Liu*, 1994; *Lobert et al.*, 1999], while more recent inventories developed for global models have relied on remote sensing products for hotspots and/or burn scars to derive area burned [*Ito and Penner*, 2004; *Hoelzemann et al.* 2004; *Simon et al.*, 2004; *Tansey et al.*, 2004; *van der Werf et al.* 2003; 2006]. Remote sensing products have also enabled better definition of temporal and spatial variations in burning, usually with monthly resolution. Both hotspot data and aerosol data have been combined with estimates of average area burned to derive the interannual variation of biomass burning for global inventories [e.g., *Schultz*, 2002; *Duncan et al.*, 2003; *Generoso et al.*, 2004; *Paton-Walsh et al.*, 2004], and estimates of daily burning for regional inventories [e.g., *Stroppiana et al.*, 2000*; Heald et al*., 2003a].

We construct here a bottom-up high-resolution emission inventory for boreal fires in North America to be tested with the ensemble of observations for CO. Recent assessments of emissions from boreal fires have relied on large fire data-bases for Alaska and Canada [*French et al.*, 2002; *Amiro et al.*, 2001; *Stocks et al.*, 2002] or on remotely sensed products, hot spots and/or burn scars, for the locations and areas of fires [e.g., *Kajii et al.*, 2002; *Kasischke et al.*, 2003, 2005; *Soja et al.*, 2004; *Sukhinin et al.*, 2004; *Giglio et al.*, 2006; *van der Werf et al.*, 2006]. Emissions are then derived by associating areas burned with fuel consumption and emission factors for individual species. These studies provide either annual or monthly estimates. Several of the studies emphasize the need to properly account for burning of the ground layer organic matter, including peat, in estimating emissions from boreal forests. Top-down approaches using atmospheric composition data have also been used recently to determine emissions from boreal fires [*e.g., Pfister et al.*, 2005].

Our inventory of Alaskan and Canadian fire emissions for 2004 is based on daily burned areas reported by NIFC (the U.S. National Interagency Fire Center). We use MODIS (Moderate Resolution Imaging Spectroradiometer) satellite hotspot data [*Justice et al.*, 2002; *Giglio et al.*, 2003] for the daily location of the fires. We combine these data with knowledge of fuel consumption and emission factors for North America. In particular we consider the burning of the ground-layer organic matter stored in the soils, important in boreal regions [e.g., *Kasischke and Penner*, 2004].

Pfister et al. [2005] previously used the MOPITT observations in a top-down inverse analysis to optimize the CO emissions from the Alaskan and Canadian wildfires for the summer of 2004. They first derived a bottom-up estimate of 13 Tg CO emitted between June and August 2004, using MODIS hotspot data to estimate area burned, and fuel consumption from the global inventory of *Ito and Penner* [2004]. Starting with this estimate as an a priori and assuming a uniform vertical distribution of the emissions between the surface and 400 hPa, their analysis yields a best a posteriori estimate of 30 ± 5 Tg for the fire emissions. We will show here that this upward adjustment can be reconciled with our best understanding of fire emissions, including in particular a large contribution from peat burning.

Peat is defined as wet, organic soil consisting mainly of partially decomposed plant material. It is produced when plant production (uptake of CO_2 from the atmosphere) is greater than the decomposition of dead plant material (release of CO_2 and CH_4 to the atmosphere). Peatlands constitute a large carbon stock and an important global sink of carbon. Peat tends to accumulate in the cool temperatures of the boreal region, as decomposition is controlled primarily by temperature. Under dry and warm conditions, the burning of peat is expected to make a large contribution to emissions from fires in boreal regions [*Zoltai et al.*, 1998; *Turetsky et al.*, 2002, 2004; *French et al.*, 2002; *Kasischke and Bruhwiler*, 2003, *Kasischke et al.*, 2005; *Soja et al*., 2004] but has not been included in standard inventories used in global models to date. We do so in our analysis by using drainage and peatland maps for Alaska and Canada, following the approach developed by *Yevich et al.* [manuscript in preparation, 2006].

Several recent studies have highlighted the importance of deep convection associated with boreal fires (so-called pyro-convection) on the distribution of aerosols and trace gases. *Fromm et al*. [2000, 2005] and *Fromm and Servranckx* [2003], show that boreal fires can have sufficient energy to trigger convection, injecting particles into the upper troposphere and even into the lower stratosphere. *Damoah et al.* [2006] identified such pyro-convective events for the Alaskan fires in 2004. In order to reproduce the transport and global dispersion of biomass burning plumes associated with these events, CTMs need to allow for injection heights well above the boundary layer [*Colarco et al.*, 2004; *Leung et al., in preparation,* 2006]. We investigate this issue here through sensitivity studies using the CO observations from 2004 to test our assumptions.

2 Daily biomass burning emission inventory

We constructed our inventory for biomass burning in the United States and Canada in 2004 by multiplying daily area burned by estimates of fuel consumption and by species-dependent emission factors per unit of fuel burned. Peat burning is considered separately, as an additional contribution [*Kasischke et al.*, 2005]. The inventory was developed with daily temporal resolution and with horizontal resolution of $1° \times 1°$.

2.1 Daily area burned

Daily area burned maps were generated by combining reports of burned areas (from the agencies that monitor the fires) with hot spots detected from space. We used the daily burned areas reported and archived by NIFC (http://www.cidi.org/wildfire), which provide summaries for the different geographic areas of the National Interagency Coordination Center (NICC), shown in Figure 1. These reports give the area burned by region, but not the specific locations of the fires. According to these reports, 5.3×10^6 ha burned in North America in June, July, and August, mainly in Alaska ($\sim 2.5 \times 10^6$ ha) and Canada (2.6×10^6 ha, of which 1.5×10^6 ha was in the Yukon Territory).

The NIFC burned areas are derived from fire perimeters. *Strawman* [2004] compares reported perimeters to information on blackened areas for several fires in the conterminous United States. They show that the reports can overestimate the burned area

by as much as 50%, and that, on average, 24% of the reported burned area did not actually burn. For the coterminous United States, we assume that 76% of the area reported actually burned. For Alaska and Canada, the fraction of unburned islands is estimated to 5% [*Amiro et al.*, 2001].

For each day and within each region of Figure 1, the area burned was distributed spatially according to the fire hot spots detected by the MODIS instruments on both the Terra and Aqua satellites [*Justice et al.*, 2002; *Giglio et al.*, 2003; *Kaufmann et al.*, 2003]. The major drawback of hot spot detection from space is obscuration by clouds. Another issue is that the hot spots could be missing part of the fire activity associated with smoldering fires [*Kasischke et al.*, 2003]. In order to minimize these effects we assume a minimum of 5-day persistence for the fires: for each day, in each 1º×1º grid square, the fire activity is defined by the maximum number of daily hotspots detected for the 5-day period centered on that day. We then use these results to spatially distribute the burned areas within the individual regions of Figure 1. Using this method, the temporal variation in burning within each NICC region is deduced from the reports, whereas the fire locations are deduced from the MODIS hotspots.

Figure 2 shows the spatial distribution of total area burned in North America during the summer of 2004. There are two major burning regions, the most important in Alaska and the Yukon, and the second in North-Central Canada. The daily variability of the area burned for each of these regions is shown in Figure 3. Fires burned in the Alaska-Yukon region during the entire summer, with the strongest burning between the end of June and mid-July, and another burning period in August. The burning in North-Central Canada region started later, with most of the area burned between mid-July and mid-August.

2.2 Fuel consumption and potential emissions

Fuel consumption in the boreal region was derived from the estimates of *Amiro et al.* [2001] for fifteen ecoclimatic zones in Canada. We included also estimates for peat burning, as described below. Fuel consumption for the coterminous United States is from *Yevich et al.* (in preparation) who allows for the three primary vegetation types (forest, woodland, grassland) for each state, based on *Brewer* [2004]. Distributions of fuel consumption for North America are shown in Figure 4.

The estimates of *Amiro et al.* [2001] include contributions from crown fires and surface burning (soil, coarse woody debris and ground vegetation). They are generally regarded as conservative and may underestimate the fuel consumption [N. French, personal communication]. Since 2004 was a severe burning season, we increased the average estimates of *Amiro et al.* for each ecozone by half of the associated standard deviation (see Table 1). For Canada the fuel consumption values were distributed on a 1°x1° map (Figure 4) using an electronic version of the ecozone map adopted by *Amiro et al*.

For Alaska, we defined three regions according to vegetation type: tundra, taiga in the Yukon Flats, and boreal forest. We used the vegetation map of *Matthews* [1983] for the location of tundra and boreal forest, and divided the forest category into the taiga in the

Yukon Flats and the western boreal forest. The Yukon Flats were specified as the forest area north of 65°N and east of 151°W. Fuel consumption was taken from *Amiro et al.* (also increased by half of the standard deviation) to allow for continuity at the border with Canada. We assume that taiga in the Yukon flats corresponds to the taiga cordillera in Canada (3.59 kg DM/m^2), and that the boreal forest in Alaska corresponds to the boreal cordillera in Canada (3.67 kg DM/m^2). For tundra in the rest of Alaska, we used 0.9 kg DM/m^2 [*Michaelson et al.*, 1996].

Amiro et al. indicate that their numbers may underestimate cases of deep burning of organic soils, especially for dry peat burning, since they did not consider peat specifically. We added the contribution from peat burning to the fuel consumption in Table 1 using distributions of the areal fraction of peat, *i.e.* the fraction of the area containing peat in each 1°×1° grid. The fraction of peat for Canada was derived from peatland maps [*Hall et al.*, 2001]. For Alaska, it was derived from a soil drainage map [*Harden et al.*, 2003], assuming that poorly drained soils are indicative of underlying peat (soil drainage classes 6 and 7). These maps indicate the burning of peat is potentially important in Alaska, the Northwest Territories, and south of Hudson Bay. According to our estimates, 17% of the reported 5.1×10^6 ha burned in Alaska and Canada were peatlands (as much as 44% in the Northwest Territories). We assumed a fuel consumption of 6.4 kg DM/ m^2 for burning in peatlands, based on the study by *Turetsky et al.* [2002]. This estimate includes all fuel burned. In order to avoid double counting, the fuel consumption per grid box was calculated by combining the value without peat (Table 1) and that including peat, depending on the areal fraction of peat for each grid box. The additional contribution from the burning of peat is shown in Figure 4.

Peat burning is expected to increase as the summer progresses, the permafrost thaws, and the soil column dries [*Turetsky et al.*, 2004; *Kasischke et al.*, 2005]. We account for this increase by applying a daily scaling factor to the peat fuel consumption, increasing linearly from zero on June 1st to two on August 31st. Since the fires started around June 15th (Figure 3), peat burning is included throughout the burning season.

For the base case (before applying the scaling factor), typical of mid-July, the fuel consumption in central Alaska is estimated to be 4.3 kg DM/m^2 on average, with some areas as high as 5.7 kg dry matter (DM)/m^2 (Figure 4). In North-Central Canada, it is estimated to be 3.6 kg DM/m^2, with values up to 6.1 kg DM/m^2. The increase of the contribution of peat during the fire season implies that the fuel consumption for fires at the end of August reaches 8 kg DM/m^2 in central Alaska and 9 kg DM/m^2 in North-Central Canada. *French et al.* [2003] estimate the average fuel consumption by fires in Alaskan boreal forests to be 3.8 kg DM/m^2, with values as high as 6.02 kg DM/m^2. *Kasischke and Johnstone* [2005] estimate that the surface fuel consumption in the black spruce forests of interior Alaska (our Yukon Flats region) range between 1.1 kg DM/m^2 and 11.3 kg DM/m^2, depending on the depth of the organic layer, the presence of permafrost and the timing of the fire. Their field studies give consumption of 1.5 and 1.9 kg DM/m^2 for two fires in June, 3.2±1.5 kg DM/m^2 for a fire in July, and 9.9±0.12 kg DM/m^2 for a fire in August. The seasonal progression is attributed to the warmer weather and thawing of permafrost. Our estimates for Alaska are consistent with these studies, but

may underestimate the most severe burning. *Stocks et al.* [2004] report 2.8–5.5 kg DM/m^2 consumed during ten experimental crown fires in jack pine-black spruce forest in the Northwest Territories, with an average of 4.3 kg DM/m^2. In this study, we use 5.1 kg DM/m^2 for the taiga plains (3.2 kg DM/m^2 without peat), which is in good agreement with the experimental data.

We combined our fuel consumption estimates with CO emission factors to construct distributions of potential emissions per unit area (*i.e.* emissions if a fire occurred). For regions south of 45°N in North America we used emission factors from *Duncan et al.* [2003]. For boreal regions, emission factors were deduced using available data from *Yokelson et al.* [1997], *Goode et al.* [2000], and the review of *Kajii et al.* [2002]. We allowed for flaming combustion, which burns mostly the above ground vegetation, and smoldering combustion, which burns mostly the organic layer, is less efficient, and releases greater quantities of CO. Following *Kasischke and Bruhwiler* [2003], we assumed 50% flaming and 50% smoldering combustion, except for peat, which was assumed to be 100% smoldering. Three vegetation types were considered, located based on the vegetation map of *Matthews* [1983]: grassland, shrub (including tundra) and forest. We used 97 g CO/kg DM for grassland and shrub [*Goode et al.*, 2000; *Kajii et al.*, 2002], and 116 g CO/kg DM for forests [*Kajii et al.*, 2002; *Kasischke and Bruhwiler*, 2003]. For peat, we used an emission factor of 239 g CO/kg DM [*Yokelson et al.*, 1997; *Kajii et al.*, 2002]. The CO emission factors and the resulting potential emissions of CO per unit area are mapped in Figure 4. In central Alaska, the potential emissions increase from 0.32 to 0.53 kg CO m^{-2} burned when peat burning is included. In North-Central Canada, the potential emissions increase from 0.3 to 0.45 kg CO m^{-2}.

2.3 Daily CO emissions

We derived CO emissions by combining potential emissions with area burned. Total emissions for summer of 2004 are shown in Figure 5, and their daily variability in the two main burning regions (Alaska-Yukon and North-Central Canada) is shown in Figure 3. The total emissions are summarized in Table 2. We estimate that the total emission of CO from biomass burning in North America was 28.6 Tg CO, of which 34% was from peat burning. For the main burning regions identified previously, Alaska-Yukon accounts for 22.1 Tg CO (27% peat), and North-Central Canada for 6.3 Tg CO (58% peat). Fires in the United States outside Alaska contributed only 0.2 Tg CO.

3 Simulation of atmospheric CO

3.1 GEOS-Chem simulation

We simulated atmospheric CO with the GEOS-Chem CTM driven by assimilated meteorological data from the Goddard Earth Observing System (GEOS-4) of the NASA Global Modeling and Assimilation Office (GMAO). We used version 7-02-04 of GEOS-Chem (http://www-as.harvard.edu/chemistry/trop/geos/) with horizontal resolution of 2° × 2.5° and 30 vertical levels from the surface to 0.01 hPa. *Bey et al.* [2001] and *Park et al.* [2004] provide a detailed description of GEOS-Chem. We conducted a CO-only

simulation in which the loss of CO by reaction with OH is calculated using archived monthly mean OH concentration fields from a detailed O_3-NO_x-VOC-aerosols simulation for 2004 [*Hudman et al.*, 2006]. The sources of CO from individual regions are tracked independently in the model. A number of previous GEOS-Chem studies have applied such CO-only simulations to constrain biomass burning emissions in different regions of the world through comparisons to atmospheric observations of CO from surface, aircraft, and satellite [*Kasibhatla et al.*, 2002; *Palmer et al.*, 2003; *Arellano et al.*, 2004; *Heald et al.*, 2004; *van der Werf et al.*, 2004].

North American sources of CO for June-August 2004 are summarized in Table 2. For the United States, we use the fossil fuel and biofuel emissions from the U.S. Environmental Protection Agency (EPA) 1999 National Emission Inventory (NEI) (http://www.epa.gov/ttn/chief/net/1999inventory.html), version 1, but with a 50% decrease in the on-road mobile sources based on data from the ICARTT aircraft campaign [*Parrish*, 2006; *Hudman et al.*, 2006]. For the rest of the world (including Canada), we use the fossil fuel emissions as described by *Bey et al.* [2001] and biofuel emissions from *Yevich and Logan* [2003]. We use the daily biomass burning inventory described in the previous section for North America. For the rest of the world, we use the monthly climatological biomass burning inventory summarized by *Lobert et al.* [1999] and *Duncan et al.* [2003], redistributed according to monthly MODIS gridded fire counts for 2004 (L. Giglio, personal communication). There were no significant Siberian fires affecting North America during the summer of 2004. The anthropogenic and biomass burning emissions are increased by 19 and 11% respectively to account for the oxidation of short-lived volatile organic compounds (VOCs) (B. N. Duncan et al., Model study of the variability and trends of carbon monoxide (1988–1997): Model formulation, evaluation and sensitivity, manuscript in preparation, 2006) (hereinafter referred to as Duncan et al., manuscript in preparation, 2006). We also include the production of CO by oxidation of methane and biogenic non-methane VOCs, with a yield of CO per molecule oxidized equal to 1 for CH_4, 30% for isoprene, 20% for monoterpenes, 1 for methanol, and 2/3 for acetone [Duncan et al., manuscript in preparation, 2006].

3.2 Injection height

Several recent studies have shown that pyro-convective events can inject emissions from boreal wildfires well above the boundary layer [*Fromm et al.* 2000, 2005; *Fromm and Servranckx*, 2003]. *Colarco et al.* [2004] showed in a CTM and trajectory analysis that an injection at 2-6 km of the emissions from Canadian wildfires in July 2002 best reproduced the observed atmospheric concentrations downwind in the northeastern United States. In their analysis of the 1998 Siberian fires using the GEOS-Chem model, *Leung et al.* [in preparation, 2006] show that injecting 60% of the emissions at 3-5 km altitude improves agreement with CO surface and column measurements. In their inverse modeling analysis of the 2004 CO fire emissions using MOPITT data, *Pfister et al.* [2005] distributed the emissions uniformly up to 400 hPa (~ 7 km), although they find that injecting CO only into the boundary layer does not affect the inversion results. No such high-altitude injection is expected for smoldering fires [*Ferguson et al.*, 2003], including peat fires.

There is evidence that strong pyro-convective events occurred in association with the 2004 Alaskan and Canadian fires. *Damoah et al.* [2006] describe events at the end of June when fire emissions penetrated into the stratosphere. Analyses of biomass burning plumes observed in the ICARTT aircraft campaign show evidence of injection into the middle and upper troposphere, as high as 10 km for some events [*de Gouw et al.*, 2006; *Kittaka et al.*, 2006].

In order to account for such events, we assume an average vertical distribution of the emissions in our standard simulation. Considering the large contribution from peat burning and smoldering combustion to the emissions, we assume that 40% of the total emissions remain in the model-diagnosed boundary layer (typically up to 800 hPa), 30% are injected in the middle troposphere up to 400 hPa, and 30% in the upper troposphere (400–200 hPa). Considerable temporal variability is in fact to be expected for injection heights, as illustrated in Figure 3 by the time series of the TOMS aerosol index (AI) [*Hsu et al*., 1996; *Herman et al.*, 1997], which is sensitive to high-altitude UV- absorbing aerosols.

4 Atmospheric observations of CO as constraints on biomass burning emissions

The inverse modeling analysis by *Pfister et al.* [2005] yields an estimate of 30 ± 5 Tg CO for the total Alaskan and Canadian CO emissions during June-August, 2004. This is a large increase over their a priori, bottom-up estimate of 13 Tg CO. Our bottom-up inventory, which uses more reliable data for area burned and fuel consumption consistent with recent field experiments, suggests that the contribution from the burning of peat (~ 9.6 Tg CO – Table 2), could explain part of this increase. We further evaluate our emission inventory here by comparing the resulting GEOS-Chem simulation with observations, and examine the sensitivity to the burning of peat and to the injection heights.

Comparisons of the GEOS-Chem surface CO with measurements from the NOAA Climate Monitoring and Diagnostics Laboratory (CMDL) network for representative northern hemisphere sites shows that the model reproduces the background level of CO (not shown). Figure 6 compares model results to the mean CO vertical distribution over eastern North America and the western North Atlantic observed during the ICARTT campaign from the NASA DC-8 aircraft covering the domain (27N-53N; 139W-36W). The model is sampled along the flight tracks (time and location). The large variability in the DC-8 observations at 6 km is due to a large fire plume encountered by the aircraft on July 18th with more than 600 ppbv CO. The fires in Alaska and Canada enhance the background CO by about 10 ppbv throughout the troposphere. However, the simulation is too high below 3 km by 10 ppbv and too low at higher altitudes by 4 ppbv.

The MOPITT observations provide a more extensive characterization of the North American fire influence. We use MOPITT measurements of CO from the Phase II version 3 of the retrieval algorithm [*Deeter et al.*, 2003], characterized by ~1 piece of information in the vertical profile at extratropical latitudes weighted towards the middle and upper troposphere [*Heald et al.*, 2003b; *Deeter et al.*, 2004]. The MOPITT retrievals

have been validated using aircraft measurements, and shown to be highly correlated with a bias of –0.5±12% for the Phase II retrievals used here [*Emmons et al.*, 2004]. The nighttime measurements have not been validated and appear biased relative to the daytime measurements [*Heald et al.*, 2004]. Therefore we consider the daytime data only. Comparisons between MOPITT observations and GEOS-Chem simulations have been shown in several studies, with focus on transpacific transport [*Heald et al.*, 2003b; *Hudman et al.*, 2004], North American pollution outflow [*Li et al.*, 2005], and derivation of sources using inverse modeling [*Arellano et al.*, 2004; *Heald et al.*, 2004]. As in these previous studies, we use the MOPITT CO column product and apply the associated averaging kernels to the model fields. A detailed description of the procedure for comparing GEOS-Chem and MOPITT CO columns is presented in *Heald et al.* [2003b, 2004].

We see from Figure 7 that the model including peatland emissions is too high over the source region of central Alaska, and too low over northeastern Canada. The latter region did not experience fires (Figure 2) and owes its high CO to long-range transport of fire plumes. Figure 8 shows the temporal variability of the average CO column over Alaska-Yukon, central Canada, and eastern North America (regions indicated on Figure 7). The timing of the main fire events is well captured by the model, demonstrating consistency between the bottom-up estimate of the daily burned areas and the MOPITT CO observations. Total CO is overestimated in the Alaska-Yukon region for the middle and end of July, and in Central Canada for the beginning of August. By contrast, the model simulation underestimates the average CO over eastern North America in July (Figure 8); the underestimate is smaller than the overestimate in the source regions, however. A possible reason is an underestimate of injection heights during the largest fires.

The variations of the TOMS AI suggests that strong pyro-convective events occurred at the end of June, the beginning of July, and in mid-July over the Alaska-Yukon region (Figure 3). We tested several assumptions for the altitude of injection, including injecting all the emissions in the boundary layer, and injecting 40% or 60% in the boundary layer. The comparisons to MOPITT data are similar when averaged over the summer. However, we find that releasing a significant fraction of the emissions into the upper troposphere gives the best simulation of the MOPITT observations downwind from the source regions for the large transport events associated with high burning periods, as illustrated in Figure 9 for mid-July. We plan to constrain CO emissions from the boreal fires along with the injection heights using an inverse modeling approach, with high time resolution.

5 Discussion and Conclusions

The 2004 fire season was one of the largest on record in Alaska and western Canada, with more than 5×10^6 ha burned. We developed a detailed inventory of fire emissions for that season, including contributions from peat burning and pyro-convection, and evaluated it using satellite (MOPITT) and in situ observations of atmospheric CO. Our inventory uses reports of area burned and MODIS satellite hotspots to reconstruct the temporal variability of daily area burned. The corresponding trace gas emissions are derived from estimates of fuel consumption and emission factors. We use drainage and

peatland maps for Alaska and Canada to account for the burning of peat. We find that 17 % of the total area burned was located in peatlands. The total emission of CO in North America is estimated to be 28.6 Tg CO, with two main burning regions: Alaska-Yukon (22.1 Tg CO) and north-central Canada (6.3 Tg CO). This is consistent with the top-down estimate of 30 ± 5 Tg CO derived by *Pfister et al.* [2005] from inverse modeling of MOPITT observations. The fires represented a major perturbation to summertime North American emissions, of the same magnitude as the anthropogenic source (18 Tg CO). Burning of peat contributes ~ 27% of total fire emissions in Alaska-Yukon and ~ 58% in Central Canada.

We incorporated our emission inventory into the GEOS-Chem CTM for comparison to atmospheric observations. In addition to the magnitude of the emissions, the sensitivity to injection height driven by pyro-convection was examined. Overall good agreement is found with MOPITT, with results sensitive to the contribution from peat burning, and to the height of injection of the emissions. The timing of the fire events is well represented. The total CO is overestimated in the Alaska-Yukon region in July. The largest fires appear to inject a large fraction of their emissions into the upper troposphere, likely because of their own heat generation.

French et al. [2004] present an analysis of uncertainties in estimates of emissions from boreal fires. They conclude that "best guess" scenarios have errors of ±25% (one standard deviation) for emissions of carbon gases, and that more field studies of fuel consumption are required. We expect that our bottom-up estimate is reliable to ±25%, as it is based on current field studies, and the agreement with MOPITT data supports this conclusion. We concur with *French et al.* [2004] and others that more field experiments to determine fuel consumption, especially burning of surface organic matter, are needed.

The injection height of emissions from boreal fires is another area of considerable uncertainty; the heights will vary with the severity of the fire and the prevailing meteorology. Aerosol height data from the Multi-angle Imaging SpectroRadiometer (MISR) instrument offer promise for assessing injection heights of smoke and gases from fires [*Kahn et al.*, 2006; *Mazzoni et al.*, 2006]. The variability of injection heights and its association with fire severity has important implications for atmospheric composition and will need to be addressed in future inverse model studies of the fire emissions.

Acknowledgments. The authors thank Rose Yevich for suggesting the use of the wetland map to define regions of peat in Alaska, and for many helpful discussions on fuel consumption. We thank L. Giglio for providing monthly gridded MODIS fire counts for 2004. This work was supported by the National Space and Aeronautics Administration Atmospheric Chemistry Modeling and Analysis Program, and by the National Science Foundation, grant ATM-0236501 (JAL and FYL).

References

Amiro, B. D., J. B. Todd, B. M. Wotton, K. A. Logan, M. D. Flannigan, B. J. Stocks, J. A. Mason, D. L. Martell, and K. G. Hirsch (2001), Direct carbon emissions from Canadian forest fires, 1959 to 1999, *Can. J. For. Res.*, 31, 512-525.

Arellano, A. F., P. S. Kasibhatla, L. Giglio, G. R. Van der Werf, and J. T. Randerson (2004), Top-down estimates of global CO sources using MOPITT measurements, *Geophys. Res. Lett.*, 31, L01104, doi:10.1029/2003GL018609.

Andreae, M., and P. Merlet, Emission of trace gases & aerosols from biomass burning (2001), *Global Biogeochem. Cycles*, 15, 955-966.

Bey, I., M. G. Schultz, D. J. Jacob, R. M. Yantosca, J. A. Logan, B. D. Field, A. M. Fiore, Q. Li, H. Y. Liu, and L. J. Mickley (2001), Global modeling of tropospheric chemistry with assimilated meteorology: Model description and evaluation, *J. Geophys. Res.*, 106(D9), 23,073–23,096.

Brewer, P., Development of the draft 2002 VISTAS emission inventory for regional haze modeling, Draft Report, (prepared by W.R.Barnard, of MACTEC Engineering and Consulting, Inc.), Feb. 10, 2004.

Colarco, P. R., M. R. Schoeberl, B. G. Doddridge, L. T. Marufu, O. Torres, and E. J. Welton, Transport of smoke from Canadian forest fires to the surface near Washington, D.C.: Injection height, entrainment, and optical properties, *J. Geophys. Res.*, 109, D06203, doi:10.1029/2003JD004248, 2004.

Crutzen, P., and M. Andreae (1990), Biomass burning in the tropics: Impact on atmospheric chemistry and biogeochemical cycles, Science, 250, 1669-1678.

Damoah R., N. Spichtinger, R. Servranckx, M. Fromm, E. W. Eloranta, I. A. Razenkov, P. James, M. Shulski, C. Forster, and A. Stohl (2006), A case study of pyro-convection using transport model and remote sensing data, *Atmos. Chem. Phys.*,6, 173-185.

DeBell, L. J., R. W. Talbot, J. E. Dibb, J. W. Munger, E. V. Fischer, and S. E. Frolking (2004), A major regional air pollution event in the northeastern United States caused by extensive forest fires in Quebec, Canada, *J. Geophys. Res.*, *109*, (D19305), doi:10.1029/2004JD004840.

Deeter, M. N., et al. (2003), Operational carbon monoxide retrieval algorithm and selected results for the MOPITT instrument, *J. Geophys. Res.*, 108(D14), 4399, doi:10.1029/2002JD003186.

Deeter, M. N., L. K. Emmons, D. P. Edwards, J. C. Gille, and J. R. Drummond (2004), Vertical resolution and information content of CO profiles retrieved by MOPITT, *Geophys. Res. Lett.*, 31, L15112, doi:10.1029/2004GL020235.

de Gouw, J. A., et al. (2006), Volatile organic compounds composition of merged and aged forest fire plumes from Alaska and western Canada, *J. Geophys. Res.*, 111, D10303, doi:10.1029/2005JD006175.

Drummond, J. R. and G.S. Mand (1996), The Measurements of Pollution in the Troposphere (MOPITT) instrument: Overall performance and calibration requirements, *J. of Atmospheric and Oceanic Technology*, *13*, 314-320.

Duncan, B.N., R.V. Martin, A.C. Staudt, R. Yevich, and J.A. Logan (2003), Interannual and Seasonal Variability of Biomass Burning Emissions Constrained by Satellite Observations, *J. Geophys. Res.*, 108(D2), 4040, doi:10.1029/2002JD002378.

Edwards, D. P., C. Halvorson and J.C. Gille (1999), Radiative transfer modeling of the EOS Terra Satellite Measurements of Pollution in the Troposphere (MOPITT) instrument, *J. Geophys. Res*., 104, 16755-16775.

Edwards, D. P., et al. (2004), Observations of carbon monoxide and aerosols from the Terra satellite: Northern Hemisphere variability, *J. Geophys. Res.*, *109*, D24202, doi:10.1029/2004JD004727.

Emmons, L. K., et al. (2004), Validation of Measurements of Pollution in the Troposphere (MOPITT) CO retrievals with aircraft and in situ profiles, *J. Geophys. Res., 109*, D03309, doi:10.1029/2003JD004101.

Ferguson, S. A., R. L. Collins, J. Ruthford, and M. Fukuda (2003), Vertical distribution of nighttime smoke following a wildland biomass fire in boreal Alaska, *J. Geophys. Res.*, 108(D23), 4743, doi:10.1029/2002JD003324.

Flannigan, M. D., and C. E. Van Wagner (1991), Climate change and wildfire in Canada, *Can. J. For. Res.*, 21, 61-72.

Forster, C., U. Wandinger, G. Wotawa, P. James, I. Mattis, D. Althausen, P. Simmonds, S. O'Doherty, S. G. Jennings, C. Kleefeld, J. Schneider, T. Trickl, S. Kreipl, H. Jäger, and A. Stohl (2001), Transport of Canadian forest fire emissions to Europe, *J. Geophys. Res.*, 106,22,887-22,906.

French, N. H. F., E. S. Kasischke, and D. G. Williams (2002), Variability in the emission of carbon-based trace gases from wildfire in the Alaskan boreal forest, *J. Geophys. Res.*, 107, 8151, doi:10.1029/2001JD000480.

French, N. H. F., P. Goovaerts, and E. S. Kasischke (2004), Uncertainty in estimating carbon emissions from boreal forest fires, *J. Geophys. Res.*, 109 (D14S08), doi:10.1029/2003JD003635.

Fromm, M., J. Alfred, K. Hoppel, J. Hornstein, R. Bevilacqua, E. Shettle, R. Servranckx, Z. Li, and B. Stocks (2000), Observations of boreal forest fire smoke in the stratosphere by POAM III, SAGE II, and lidar in 1998, *Geophys. Res. Lett.*, 27, 1407-1410.

Fromm, M. and R. Servranckx (2003), Transport of forest fire smoke above the tropopause by supercell convection, *Geophys. Res. Lett.*, 30(10), 1542, doi:10.1029/2002GL016820.

Fromm, M., R. Bevilacqua, R. Servranckx, J. Rosen, J. P. Thayer, J. Herman, and D. Larko (2005), Pyro-cumulonimbus injection of smoke to the stratosphere: Observations and impact of a super blowup in northwestern Canada on 3–4 August 1998, *J. Geophys. Res.*, 110, D08205, doi:10.1029/2004JD005350.

Generoso, S., F.-M. Bréon, Y. Balkanski, O. Boucher, and M. Shulz (2003), Improving the seasonal cycle and interannual variations of biomass burning aerosol sources, *Atm. Chem. Phys.*, 1973-1989.

Giglio, L., J. Descloitres, C. O. Justice, and Y. J. Kaufman (2003), An enhanced contextual fire detection algorithm for MODIS, *Remote Sens. Environ.*, 87, 273-282.

Giglio, L. , G. R. van der Werf, J. T. Randerson, G. J. Collatz, and P. Kasibhatla (2006), Global estimation of burned area using MODIS active fire observations, *Atmosph. Chem. Phys.*, 6, 957-974.

Gillett, N. P., A. J. Weaver, F. W. Zwiers, and M. D. Flannigan (2004), Detecting the effect of climate change on Canadian forest fires, *Geophys. Res. Lett., 31*, L18211, doi:10.1029/2004GL020876.

Goode, J. G., R. J. Yokelson, D. E. Ward, R. A. Susott, R. E. Babbitt, M. A. Davies, and W. M. Hao (2000), Measurements of excess O_3, CO_2, CH_4, C_2H_4, C_2H_2, HCN, NO, NH_3, HCOOH, CH_3COOH, HCHO, and CH_3H in 1997 Alaskan biomass burning plumes by airborne Fourier transform infrared spectroscopy (AFTIR), *J. Geophys. Res.*, 105(D17), 22,147–22,166.

Hall, F., G. Rapalee, and D. Knapp (2001), BOREAS Follow-On DSP-10, Regridded Peatland Maps. Data set. Available on-line (http://www.daac.ornl.gov) from Oak Ridge National Laboratory Distributed Active Archive Center, Oak Ridge, Tennessee, U.S.A.

Hao, W. M., and M.-H. Liu (1994), Spatial and temporal distribution of tropical biomass burning, *Global Biogeochem. Cycles.*, 8, 495-503.

Harden, J.W., R. Meier, C. Darnel, D. K. Swanson, and A.D. McGuire (2003), Soil drainage and its potential for influencing wildfire in Alaska, in Studies in Alaska by the U.S. Geological Survey. J Galloway (ed.), U.S. Geological Survey Professional Paper 1678.

Heald, C.L., D.J. Jacob, D.B.A. Jones, P.I. Palmer, J.A. Logan, D.G. Streets, G.W. Sachse, J.C. Gille, R.N. Hoffman, and T. Nehrkorn (2004), Comparative inverse analysis of satellite (MOPITT) and aircraft (TRACE-P) observations to estimate Asian sources of carbon monoxide, *J. Geophys. Res.*, 109, (D23), D23306, doi:10.1029/2004JD005185.

Heald, C.L., D.J. Jacob, P.I. Palmer, M.J. Evans, G.W. Sachse, H.B. Singh and D.R. Blake (2003a), Biomass burning emission inventory with daily resolution: application to aircraft observations of Asian outflow, *J. Geophys. Res., 108* (D21), 8811, doi:10.1029/2002JD003082.

Heald, C.L., D.J. Jacob, A.M. Fiore, L.K. Emmons, J.C. Gille, M.N. Deeter, J. Warner, D.P. Edwards, J.H. Crawford, A.J. Hamlin, G.W. Sachse, E.V. Browell, M.A. Avery, S.A. Vay, D.J. Westberg, D. R.Blake, H.B.Singh, S.T. Sandholm, R.W. Talbot, H.E. Fuelberg (2003b), Asian outflow and transpacific transport of carbon monoxide and ozone pollution: An integrated satellite, aircraft and model perspective, *J. Geophys. Res.*, 108 (D24), 4804, doi:10.1029/2003JD003507.

Herman, J. R., P. K. Bhartia, O. Torres, C. Hsu, C. Seftor, and E. Celarier (1997), Global distribution of UV-absorbing aerosols from Nimbus 7/TOMS data, *J. Geophys. Res.*, 102(D14), 16,911–16,922.

Hoelzemann J. J., M. G. Schultz, G. P. Brasseur, C. Granier, and M. Simon (2004), The Global Wildland fire Emission Model GWEM: evaluating the use of global area burnt satellite data, *J. Geophys. Res*., 109, D14S04, doi:10.1029/2003JD003666.

Honrath, R. E., R. C. Owen, M. Val Martin, J. S. Reid, K. Lapina, P. Fialho, M. P. Dziobak, J. Kleissl, and D. L. Westphal (2004), Regional and hemispheric impacts of anthropogenic and biomass burning emissions on summertime CO and O3 in the North Atlantic lower free troposphere, *J. Geophys. Res.*, 109, D24310, doi:2004JD005417.

Hsu, N. C., J. R. Herman, P. K. Bhartia, C. J. Seftor, O. Torres, A. M. Thompson, J. F. Gleason, T. F. Eck, and B. N. Holben (1996), Detection of biomass burning smoke from TOMS measurements, *Geophys. Res. Lett.*, 23, 745-748.

Hudman, R. C., D. J. Jacob, O. C. Cooper, M. J. Evans, C. L. Heald, R. J. Park, F. Fehsenfeld, F. Flocke, J. Holloway, G. Hubler, K. Kita, M. Koike, Y. Kondo, A. Neuman, J. Nowak, S. Oltmans, D. Parrish, J. M. Roberts, T. Ryerson (2004), Ozone production in transpacific Asian pollution plumes and implications for ozone air quality in California, *J. Geophys. Res.*, 109, D23S10,10.1029/2004JD004974.

Hudman et al. (2006), Surface and lightning sources of nitrogen oxides in the United States: magnitudes, chemical evolution and outflow, in preparation for *J. Geophys. Res.*

Ito, A., and J. E. Penner, Global estimates of biomass burning emissions based on satellite imagery for the year 2000 (2004), *J. Geophys. Res.*, 109, D14S05, doi:10.1029/2003JD004423.

Jaffe, D., I. Bertschi, L. Jaegle, P. Novelli, J. S. Reid, H. Tanimoto, R. Vingarzan, and D. L. Westphal (2004), Long-range transport of Siberian biomass burning emissions and impact on surface ozone in western North America, *Geophys. Res. Lett.*, 31, L16106, doi:10.1029/2004GL020093.

Justice, C. O., L. Giglio, S. Korontzi, J. Owens, J. T. Morisette, D. Roy, J. Descloitres, S. Alleaume, F. Petitcolin, and Y. J. Kaufman (2002), The MODIS fire products, *Remote Sens. Environ.*, 83, 244-262.

Kahn, R. A., W.-H. Li, C. Moroney, D. D. Diner, J. V. Martonchik, and E. Fishbein (2006), Aerosol characterization from space-based multi-angle imaging, *J. Geophys. Res.*, submitted.

Kajii, Y., et al. (2002), Boreal forest fires in Siberia in 1998: Estimation of area burned and emissions of pollutants by advanced very high resolution radiometer satellite data, *J. Geophys. Res.*, 107(D24), 4745, doi:10.1029/2001JD001078.

Kasibhatla, P.S., A. Arellano, J.A. Logan, P.I. Palmer, and P. Novelli (2003), Top-down estimate of a large source of atmospheric carbon monoxide associated with fuel combustion in Asia, *Geophys. Res. Lett.*, 29(19),1900, doi:10.1029/2002GL015581.

Kasischke, E. S., J. H. Hewson, B. Stocks, G. van der Werf, and J. Randerson (2003), The use of ATSR active firecounts for estimating relative patterns of biomass burning – a study from the boreal forest region, *Geophys. Res. Lett.*, 30(18), 1969, doi:10.1029/2003GL017859.

Kasischke, E.S., and L.M. Bruhwiler (2003), Emissions of carbon dioxide, carbon monoxide and methane from boreal forest fires in 1998, *J. Geophys. Res.*, 108 (D1), 8146, doi:10.1029/2001JD000461.

Kasischke, E. S., and J. E. Penner (2004), Improving global estimates of atmospheric emissions from biomass burning, *J. Geophys. Res*., 109 (D14S01), doi:10.1029/2004JD004972.

Kasischke, E. S., E. J. Hyer, P. C. Novelli, L. P. Bruhwiler, N. H. F. French, A; I. Sukhinin, J. H. Hewson, and B. J. Stocks (2005), Influence of boreal fire emissions on Northern Hemisphere atmospheric carbon and carbon monoxide, *Global Biogeochem. Cycles*, 19 (1), GB1012, 10.1029/2004GB002300**.**

Kasischke, E. S., and J. F. Johnstone (2005), Variation in postfire organic layer thickness in a black spruce forest complex in interior Alaska and its effects on soil temperature and moisture, *Can. J. For. Res.*, 35(9), 2164-2177.

Kaufman, Y. J., C. Ichoku, L. Giglio, S. Korontzi, D. A. Chu, W. M. Hao, R.-R. Li, and C. O. Justice (2003), Fire and smoke observed from the Earth Observing System MODIS instrument–products, validation, and operational use, *Int. J. Remote Sensing*, 24, 8, 1765-1781.

Kittaka et al. (2006), An aerosol model study with MODIS AOD assimilation: Assessing impacts of Alaskan smoke on the continental US air quality during ICARTT/INTEX-NA, in preparation for J. *Geophys. Res*.

Kurz, W.A., and M.J. Apps (1999), A 70-year retrospective analysis of carbon fluxes in the Canadian forest sector, *Ecological Applications*, 9(2):526–547.

Leung, F.-Y., et al. (2006), Impacts of enhanced biomass burning in the boreal forests in 1998 on tropospheric chemistry and the sensitivity of model results to injection height, in preparation for *J. Geophys. Res.*

Li, Q., D. J. Jacob, R. Park, Y. Wang, C. L. Heald, R. Hudman, R. M. Yantosca, R. V. Martin, and M. Evans (2005), North American pollution outflow and the trapping of convectively lifted pollution by upper-level anticyclone, *J. Geophys. Res.*, 110, D10301, doi:10.1029/2004JD005039.

Liousse, C., J. E. Penner, C. Chuang, J. J. Walton, H. Eddleman, and H. Cachier (1996), A global three-dimensional model study of carbonaceous aerosols, *J. Geophys. Res., 101*(D14), 19,411–19,432.

Lobert, J. M., W. C. Keene, J. A. Logan, and R. Yevich (1999), Global chlorine emissions from biomass burning: Reactive chlorine emission inventory, *J. Geophys. Res., 104*, 8373-8389.

Logan J. A., J. M. Prather, S. C. Wofsy, and M.B. McElroy (1981), Tropospheric chemistry: a global perspective. *J. Geophys. Res., 86*, 7210-7254.

Matthews, E. (1983), Global vegetation and land use: new high-resolution data bases for climate studies, *J. Climate and Applied Meteorology, 22,* 474-487.

Mazzoni, D. D. Diner, R. Kahn, Q. Li, L. Tong, and J. A. Logan (2006), A data-mining approach to associating MISR smoke plume heights with MODIS fire measurements, *Remote Sens. Environ.*, submitted.

McKeen, S. A. et al. (2002), Ozone production from Canadian wildfires during June and July of 1995, *J. Geophys. Res., 107(D14),* 4192, doi:10.1029/2001JD000697.

Michaelson, G.J., C.L. Ping, and J.M. Kimble (1996), Carbon Storage and Distribution in Tundra Soils of Arctic Alaska, U.S.A., *Arctic and Alpine Research*, 28, 4, 414-424.

Novelli, P. C., K. A. Masarie, P. M. Lang, B. D. Hall, R. C. Myers, and J. W. Elkins (2003), Reanalysis of tropospheric CO trends: Effects of the 1997–1998 wildfires, *J. Geophys. Res.*, 108(D15), 4464, doi:10.1029/2002JD003031.

Palmer, P.I., D.J. Jacob, D.B.A. Jones, C.L. Heald, R.M. Yantosca, J.A. Logan, G.W. Sachse, and D.G. Streets (2003), Inverting for emissions of carbon monoxide from Asia using aircraft observations over the western Pacific, *J. Geophys. Res.*, 108(D21), 8828, doi:10.1029/2003JD003397.

Park, R. J., D. J. Jacob, B. D. Field, R. M. Yantosca, and M. Chin (2004), Natural and transboundary pollution influences on sulfate-nitrate-ammonium aerosols in the United States: implications for policy , *J. Geophys. Res.*, D15204, 10.1029/2003JD004473.

Parrish, D.D. (2006), Critical evaluation of U.S. on-road vehicle emission inventories, *Atmospheric Environment, in press*.

Paton-Walsh, C., N. Jones, S.R. Wilson, A. Meier, N. Deutscher, D.W.T. Griffith, R. Mitchell, and S. Campbell (2004), Trace Gas Emissions from Biomass Burning inferred from Aerosol Optical Depth, *Geophys. Res. Lett.*, 31, L05116, doi :10.1029/2003GL018973.

Pfister, G., P. G. Hess, L. K. Emmons, J.-F. Lamarque, C. Wiedinmyer, D. P. Edwards, G. Pétron, J. C. Gille, and G. W. Sachse (2005), Quantifying CO emissions from the 2004 Alaskan wildfires using MOPITT CO data, *Geophys. Res. Lett.*, 32, L11809, doi:10.1029/2005GL022995.

Sachse, G. W., G. F. Hill, L. O. wade, and M. G. Perry (1987), Fast-response, high-precision carbon-monoxide sensor using a tunable diode-laser absorption technique, *J. Geophys. Res.*, 92, 2071-2081.

Schultz, M. G. (2002), On the use of ATSR fire count data to estimate the seasonal and interannual variability of vegetation fire emissions, *Atmos. Chem. Phys.*, 2, 387–395.

Seiler, W. and P.J. Crutzen (1980), Estimates of gross and net fluxes of carbon between the biosphere and the atmosphere from biomass burning. *Climatic Change*, 2, 207-247.

Simon, M., S. Plummer, F. Fierens, J. J. Hoelzemann, and O. Arino (2004), Burnt area detection at global scale using ATSR-2: the GLOBSCAR products and their qualification, *J. Geophys. Res., 109*, D14S02, doi:10.1029/2003JD003622.

Soja, A.J., W. R. Cofer, H. H. Shugart, A. I. Sukhinin, P. W. Stackhouse Jr., D. J. McRae, and S. G. Conard (2004), Estimating Fire Emissions and Disparities in Boreal Siberia (1998-2002), *J. Geophys. Res.*, 109 (D14S06), doi:10.1029/2004JD004570.

Stocks, B. J., M. A. Fosberg, T. J. Lynham, L. Mearns, B. M. Wotton, Q. Yang, J.-Z. Jin, K. Lawrence, G. R. Hartley, J. A. Mason, and D. W. McKenney (1998), Climate change and forest fire potential in Russian and Canadian boreal forests, *Climatic Change*, 38, 1-13.

Stocks, B. J., et al. (2002), Large forest fires in Canada, 1959–1997, *J. Geophys. Res.*, 108(D1), 8149, doi:10.1029/2001JD000484.

Stocks, B. J., M.E. Alexander, B.M. Wotton, C.N. Stefner, M.D. Flannigan, S.W. Taylor, N. Lavoie, J.A. Mason, G.R. Hartley, M.E. Maffey, G.N. Dalrymple, T.W. Blake, M.G. Cruz, and R.A. Lanoville (2004), Crown fire behaviour in a northern jack pine – black spruce forest, *Can. J. For. Res.*, 34, 1548–1560, doi: 10.1139/X04-054.

Stohl, A. (2006a), Characteristics of atmospheric transport into the Arctic troposphere, *J. Geophys. Res.*, 111, D11306, doi:10.1029/2005JD006888.

Stohl, A., et al. (2006b), Pan-Arctic enhancements of light absorbing aerosol concentrations due to North American boreal forest fires during summer 2004, in preparation for J. Geophys. Res.

Strawman (2004), Approach for technical refinement of large fires and fire complexes for wrap phase I fire emissions inventory, technical memorandum, Air Sciences Inc.

Stroppiana, D., S. Pinnock, and J.-M. Gregoire (2000), The Global Fire Product: daily fire occurrence, from April 1992 to December 1993, derived from NOAA-AVHRR data, *Int. J. Remote Sensing*, *21*, 6/7, 1279-1288.

Sukhinin, A. I., N. H. F. French, E. S. Kasischke, J. H. Hewson, A. J. Soja, I. A. Csiszar, E. J. Hyer, T. Loboda, S. G. Conard, V. I. Romasko, E. A. Pavlichenko, S. I. Miskiv, and O. A. Slinkina (2004), AVHRR-based mapping of fires in Russia: New Products for fire Management and carbon cycle studies, *Remote Sensing Env.*, 93:546-564, doi:10.1016/j.rse.2004.08.011.

Tansey, K., et al. (2004), Vegetation burning in the year 2000: Global burned area estimates from SPOT VEGETATION data, *J. Geophys. Res.*, 109, D14S03, doi:10.1029/2003JD003598.

Turetsky, M., K. Wieder, L. Halsey, and D. Vitt (2002), Current disturbance and the diminishing peatland carbon sink, *Geophys. Res. Lett.*, 29 (11), 1526, doi:10.1029/2001GL014000.

Turetsky, M. R., B. D. Amiro, E. Bosch, and J. S. Bhatti (2004), Historical burn area in western Canadian peatlands and its relationship to fire weather indices, *Global Biogeochem. Cycles*, 18, GB4014, doi:10.1029/2004GB002222.

Van der Werf, G.R., J.T. Randerson, G.J. Collatz, and L. Giglio (2003), Carbon emissions from fires in tropical and subtropical ecosystems, *Global Change Biology*, 9, 547-562.

Van der Werf, G. R., J. T. Randerson, G. J. Collatz, L. Giglio, P. S. Kasibhatla, A. F. Arellano Jr., S. C. Olsen, and E. S. Kasischke (2004), Continental-scale partitioning of fire emissions during the 1997 to 2001 El Niño/La Niña period, *Science*, 303, 73-76.

Van der Werf, G. R., J. T. Randerson, L. Giglio, G. J. Collatz, P. S. Kasibhatla, and A. F. Arellano Jr. (2006), Interannual variability of global biomass burning emissions from 1997 to 2004, *Atmos. Chem. Phys. Discuss.*, 6, 3175–3226.

Whitlock, C. (2004), Forests, Fires and Climate, *Nature*, 432, 28-29.

Wotawa, G., and M. Trainer (2000), The Influence of Canadian Forest Fires on Pollutant Concentrations in the United States, *Science*, 288, 324-328.

Wotawa, G., P. C. Novelli, M. Trainer, and C. Granier (2001), Inter-annual variability of summertime CO concentrations in the Northern Hemisphere explained by boreal forest fires in North America and Russia, *Geophys. Res. Lett.*, 28(24), 4575-4578, 10.1029/2001GL013686.

Yevich, R., and J. A. Logan (2003), An assesment of biofuel use and burning of agricultural waste in the developing world, *Global Biogeochem. Cycles, 17 (4)*, 1095, doi:10.1029/2002GB001952.

Yokelson, R. J., R. Susott, D. E. Ward, J. Reardon, and D. W. T. Griffith (1997), Emissions from smoldering combustion of biomass measured by open-path Fourier transform infrared spectroscopy, *J. Geophys. Res.*, 102(D15), 18,865–18,878.

Yurganov, L. N., et al. (2004), A quantitative assessment of the 1998 carbon monoxide emission anomaly in the Northern Hemisphere based on total column and surface concentration measurements, *J. Geophys. Res.*, 109, D15305, doi:10.1029/2004JD004559.

Zoltai, S. C., L. A. Morrissey, G. P. Livingston, and W. J. de Groot (1998), Effects of fire on carbon cycling in North American boreal peatlands, *Env. Rev.*, 6, 13– 24.

Table 1 – Fuel consumption for the each ecozone in Canada.

Ecozone	Fuel consumption (kg DM/m^2)[a]
Southern Arctic	2.70
Taiga plains	3.23
Taiga shield West	2.20
Taiga shield East	2.28
Boreal shield West	2.88
Boreal shield East	2.38
Atlantic Maritime	2.13
Mixedwood plains	1.89
Boreal plains	2.84
Prairies	1.46
Taiga Cordillera	3.59
Boreal Cordillera	3.67
Pacific Maritime	3.78
Montane Cordillera	4.43
Hudson plains	2.22

a. The values were derived from the mean fuel consumption given by *Amiro et al.* [2001] for fires in 1959-1999 by adding half of the standard deviation for each ecozone.

Table 2- North American CO sources (Tg CO) for June-August 2004[(a)]

	Biomass burning		Anthropogenic	Biogenic
	Non peat	Peat		
Contiguous USA	0.2		14.2	14.1
Alaska	9.5	5.6	0.02	0.7
Canada	9.3	4.0	3.8	7.2
Total North America	19.	9.6	18	22.

(a) Including the contribution from the oxidation of short-lived VOCs

Figure captions

Figure 1 – NICC geographic regions for which total areas burned are reported daily (http://www.nifc.gov/nicc/).

Figure 2 – Total area burned for the summer of 2004 (June-July-August) on the $1° \times 1°$ model grid.

Figure 3 – Daily variability between June 1st and August 31st, 2004, of area burned (top panels), and of the derived CO emissions (middle panels) with and without considering the contribution of peat burning (solid and dotted lines respectively). The bottom panel shows the maximum value of the TOMS aerosol index in each region (http://toms.gsfc.nasa.gov/aerosols/aerosols_v8.html).

Figure 4 – Fuel consumption, CO emission factors, and potential emissions of CO without including peat (left) and additional contribution from peat burning, depending on the areal fraction of peat (right). "DM" denotes dry matter.

Figure 5 – Biomass burning CO emissions for June-August 2004, separating the contribution from peat burning.

Figure 6 – Vertical profiles of CO over eastern North America and the western North Atlantic during the summer 2004 ICARTT aircraft campaign. Observations from the DC-8 aircraft [*Sachse et al.*, 1987] (dots, dotted line) are compared to model results sampled along the flight tracks (solid line). The model simulation without contributions from biomass burning in Alaska and Canada is also indicated (dashed line). The error bars correspond to the standard deviation in the observations at each level.

Figure 7 – Top panels: MOPITT total column CO for June-August 2004 averaged on the 2ºx2.5º horizontal grid of the GEOS-Chem model, and number of days of observation included in the average. The boxes on the top left panel show the regions used for the evaluation of the total CO temporal variability during the summer of 2004 (Figure 9). Bottom panels: corresponding GEOS-Chem simulations with and without peat burning (MOPITT averaging kernels have been applied to the model fields).

Figure 8 – Time series of the averaged total columns of CO over 3 regions (see Figure 7) during the summer of 2004, as observed by MOPITT (solid line) and as simulated by GEOS-Chem (dashed-dotted line). Also shown are GEOS-Chem results not including peat burning (dotted line).

Figure 9 – MOPITT total column CO averaged for July 15-18 2004 on the 2ºx2.5º horizontal grid of the GEOS-Chem model, and corresponding GEOS-Chem simulations (with peat burning included) using three different parameterizations of the injection height of the fire emissions: 100% in the model-diagnosed boundary layer (BL); 40% in the boundary layer and 60 % in the middle troposphere (MT) up to 400 hPa; and 40% in the boundary layer, 30% in the middle troposphere, 30% in the upper troposphere (UT) at 400-200 hPa (standard simulation).

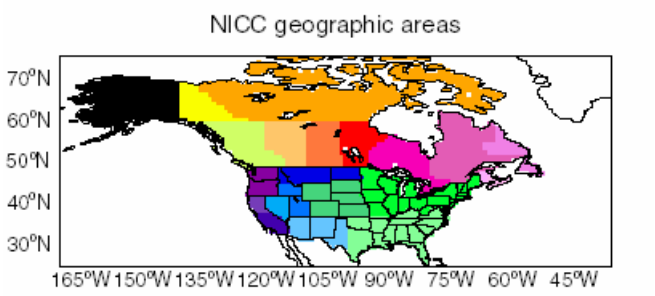

Figure 1 – NICC geographic regions for which total areas burned are reported daily (http://www.nifc.gov/nicc/).

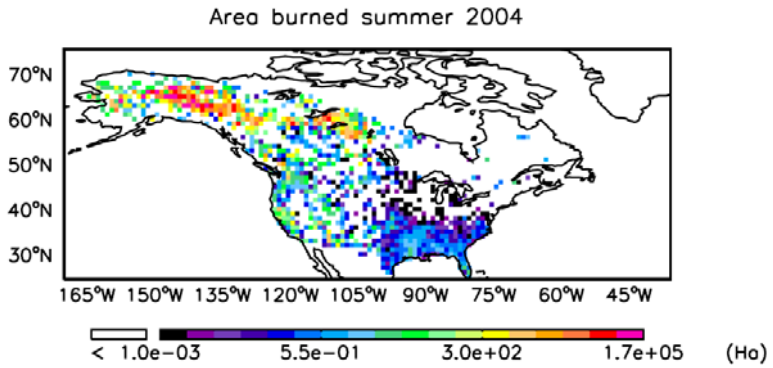

Figure 2 – Total area burned for the summer of 2004 (June-July-August) on the 1°×1° model grid.

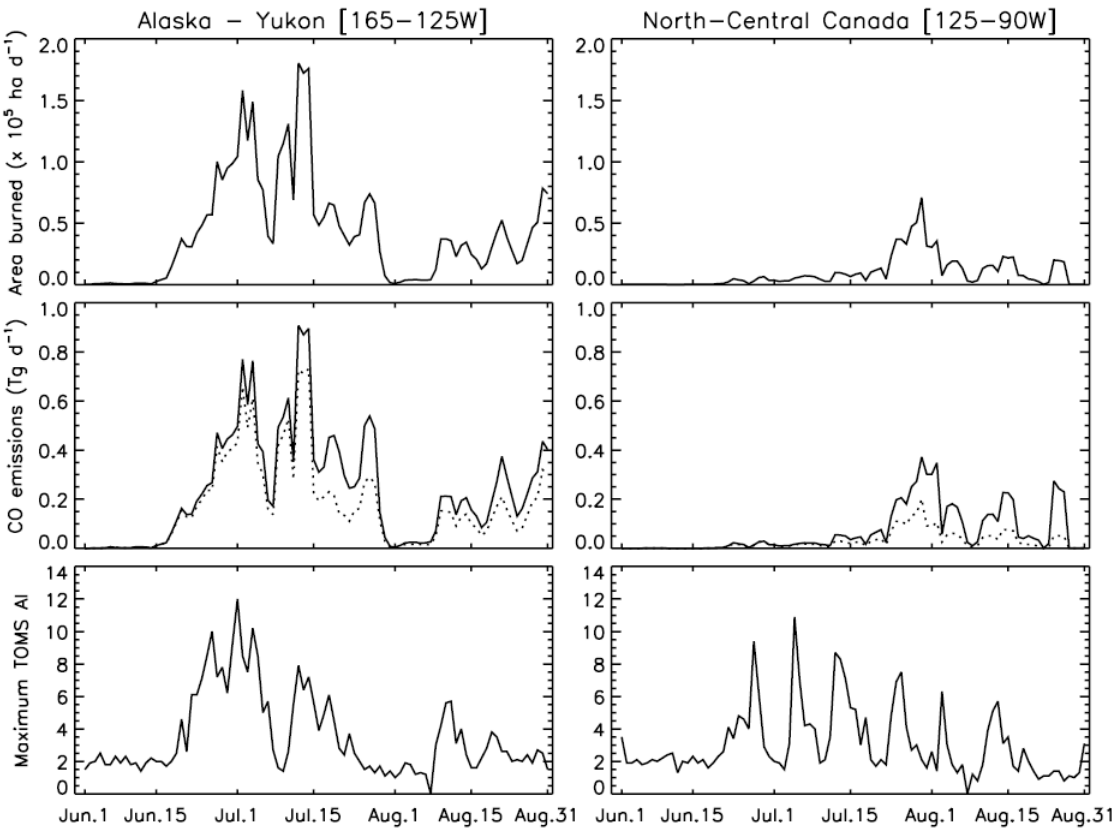

Figure 3 – Daily variability between June 1st and August 31st, 2004, of area burned (top panels), and of the derived CO emissions (middle panels) with and without considering the contribution of peat burning (solid and dotted lines respectively). The bottom panel shows the maximum value of the TOMS aerosol index in each region (http://toms.gsfc.nasa.gov/aerosols/aerosols_v8.html).

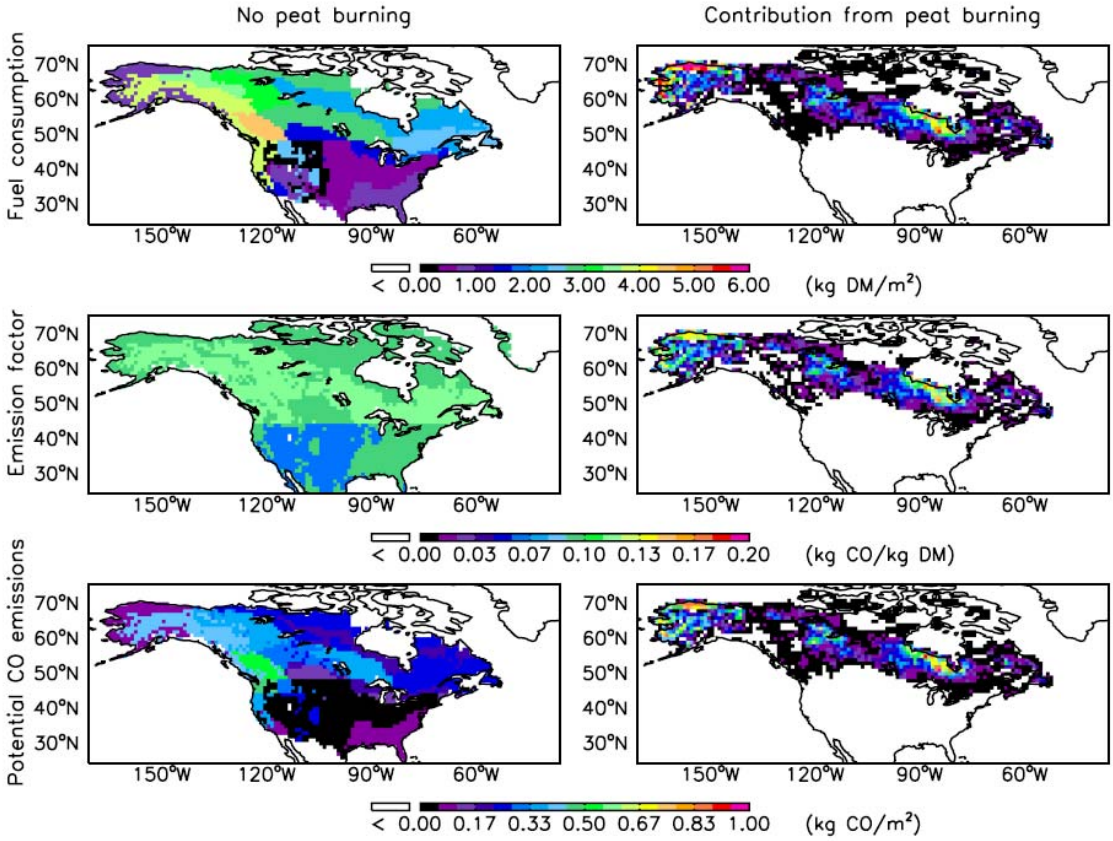

Figure 4 – Fuel consumption, CO emission factors, and potential emissions of CO without including peat (left) and additional contribution from peat burning, depending on the areal fraction of peat (right). “DM” denotes dry matter.

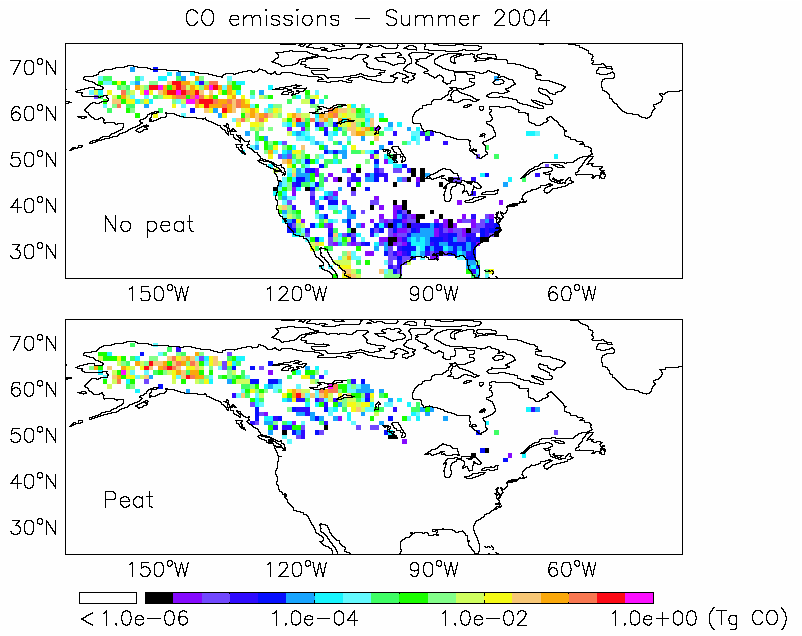

Figure 5 – Biomass burning CO emissions for June-August 2004, separating the contribution from peat burning.

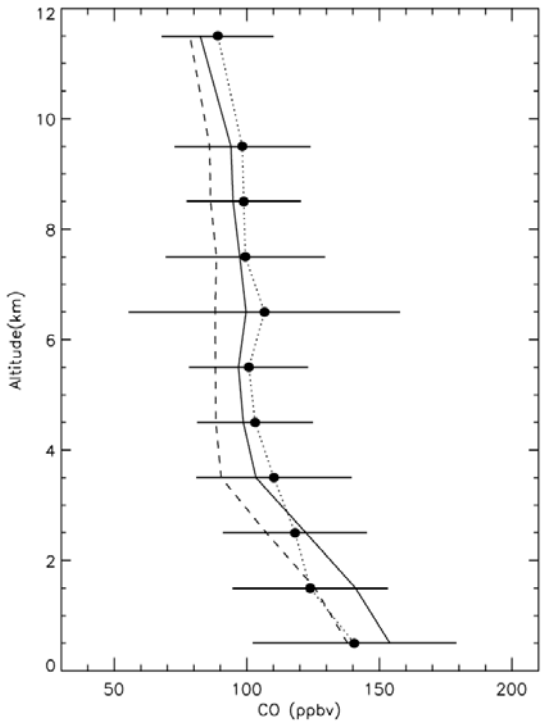

Figure 6 – Vertical profiles of CO over eastern North America and the western North Atlantic during the summer 2004 ICARTT aircraft campaign. Observations from the DC-8 aircraft (dots, dotted line) are compared to model results sampled along the flight tracks (solid line). The model simulation without contributions from biomass burning in Alaska and Canada is also indicated (dashed line). The error bars correspond to the standard deviation in the observations at each level.

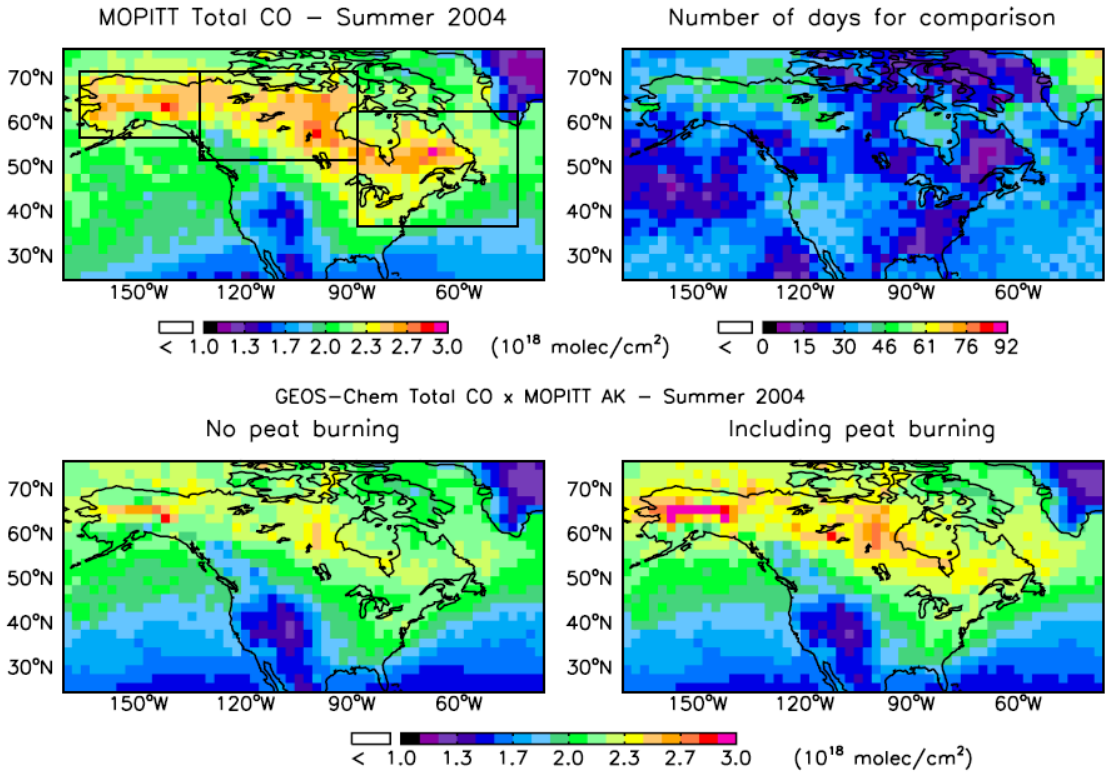

Figure 7 – Top panels: MOPITT total column CO for June-August 2004 averaged on the 2ºx2.5º horizontal grid of the GEOS-Chem model, and number of days of observation included in the average. The boxes on the top left panel show the regions used for the evaluation of the total CO temporal variability during the summer 2004 (Figure 9). Bottom panels: corresponding GEOS-Chem simulations with and without peat burning (MOPITT averaging kernels have been applied to the model fields).

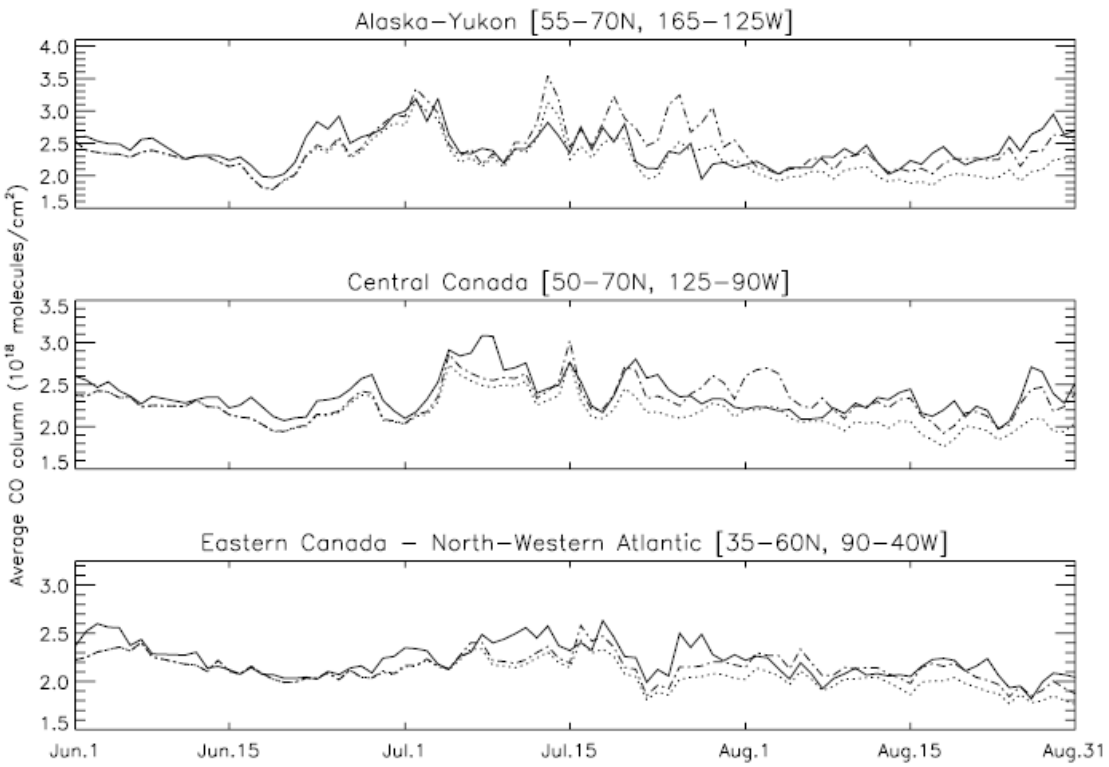

Figure 8 – Time series of the averaged total columns of CO over 3 regions (see Figure 7) during the summer 2004, as observed by MOPITT (solid line) and as simulated by GEOS-Chem (dashed-dotted line). Also shown are GEOS-Chem results not including peat burning (dotted line).

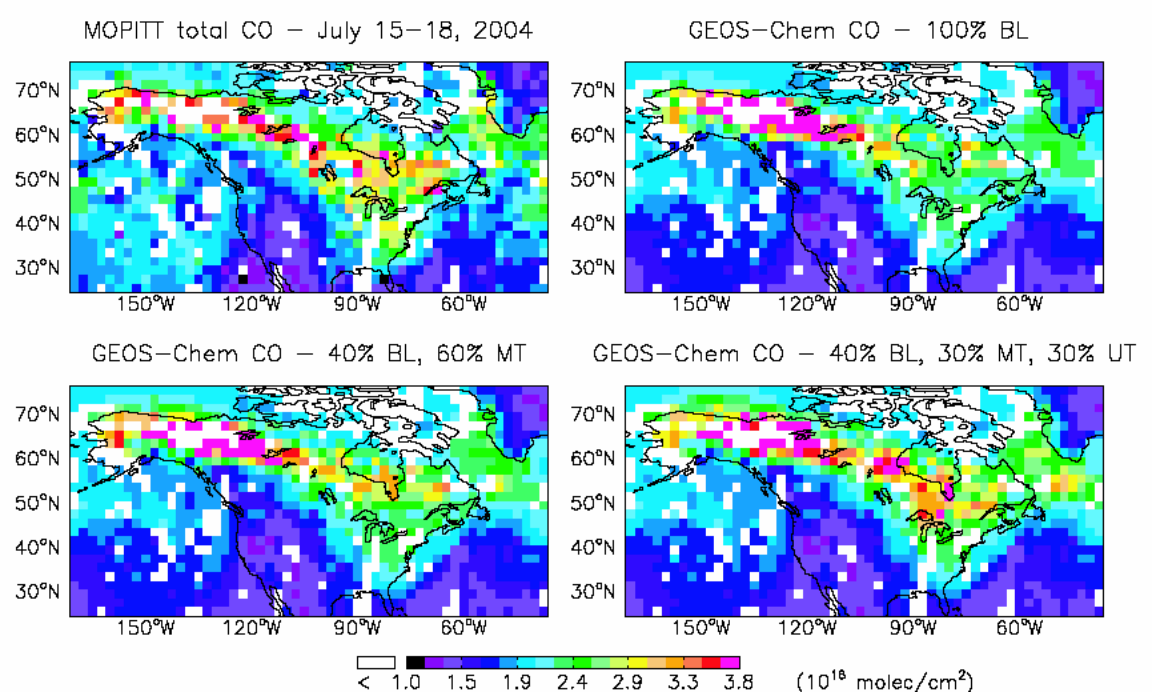

Figure 9 – MOPITT total column CO averaged for July 15-18 2004 on the 2°x2.5° horizontal grid of the GEOS-Chem model, and corresponding GEOS-Chem simulations (with peat burning included) using three different parameterizations of the injection height of the fire emissions: 100% in the model-diagnosed boundary layer (BL); 40% in the boundary layer and 60 % in the middle troposphere (MT) up to 400 hPa; and 40% in the boundary layer, 30% in the middle troposphere, 30% in the upper troposphere (UT) at 400-200 hPa (standard simulation).